Biomedical Signal Processing and Control 68 (2021) 102683

Contents lists available at ScienceDirect

Biomedical Signal Processing and Control

journal homepage: www.elsevier.com/locate/bspc

Near real-time single-beat myocardial infarction detection from single-lead electrocardiogram using Long Short-Term Memory Neural Network☆

Harold Martin [a], Walter Izquierdo [a], Mercedes Cabrerizo [a], Anastasio Cabrera [b], Malek Adjouadi [a,*]

[a] CATE, Department of Electrical and Computer Engineering, Florida International University, Miami, FL, USA
[b] Manatee Memorial Hospital, Bradenton, FL, USA

ARTICLE INFO

Keywords:
Cardiovascular disease
Electrocardiograms
Long Short-Term Memory Neural Network
Myocardial infarction
Real-time processing

ABSTRACT

This study proposes a novel Long Short-Term Memory Neural Network (LSTM) architecture for the diagnosis of myocardial infarctions from individual heartbeats of single-lead electrocardiograms (ECGs). The proposed model is trained using an unbiased patient split approach and validated using 10-fold cross-validation over 148 myocardial infarction and 52 Healthy Control patients from the Physikalisch-Technische Bundesanstalt diagnostic ECG Database to generate an inter-patient classifier. We further demonstrate why special care must be taken when generating the training and testing datasets by exploring the effects of various data-split techniques that could mask the occurrence of overfitting and produce misleadingly high testing metrics of the model's performance. A thorough assessment of these results is provided using several standard metrics for different data split methods to show their tendency to overfitting, data leakage, and bias introduced from previously seen heart beats during the training phase. The design achieves near real-time diagnosis of 40 ms while providing an accuracy of 89.56% (with a 95% Confidence Interval (CI) of ±2.79%), recall/sensitivity of 91.88% (±3.13% 95% CI), and a specificity of 80.81% (±9.62% 95%CI). The fast processing makes the model readily deployable on currently existing mobile devices and testing instruments. The achieved performance makes the proposed method a new research direction for attaining real-time and unbiased diagnosis. While, the modular architectural design of the LSTM network structure, which is amenable for the inclusion of other ECG leads, could serve as a platform for early detection of myocardial infarction and for the planning of early treatment(s).

1. Introduction

According to the Center for Disease Control and Prevention (CDC), every 40 seconds someone in the USA suffers from a heart attack. There are roughly 790 thousand myocardial infarctions per year in the United States (although some sources list this number to be even higher) and about 20% of them occur without warning or symptoms [1]. Altogether, 49 percent of Americans have relevant risk factors of heart diseases that could lead to myocardial infarctions at an average medical cost of $11, 664 [2,3]. Therefore, as they remain a condition with significant possible complications [4], their accurate and early diagnosis is of utmost importance and necessity.

Electrocardiograms (ECGs) are a powerful tool used by physicians to diagnose heart defects and abnormalities by looking into the heart's electrical activity and assess vital information about the organ's health [5]. Therefore, numerous papers have used the information present therein to attempt and diagnose myocardial infarctions and other cardiac diseases [6–38]. As could be expected, the source of the information being processed (ECG lead(s)) and the classification method used vary, yielding varied results in terms of the different performance measures. Three main types of data splits (beat split, file or record split and patient split) are well reported in the literature, relying essentially on two distinct types of classifiers, namely intra- and inter-patient classifiers, which are detailed in the "Data" section.

The authors of [26] use deep convolutional neural networks to detect myocardial infarctions using single lead ECGs (lead II) producing an intra-patient classifier. Padmavathi Kora in [7] uses a Hybrid Firefly algorithm to perform feature extraction to be then fed into either a

☆ This work was support by the National Science Foundation under grants: CNS-1920182, CNS-1551221, and CNS-1532061. The generous support of the Ware Foundation is greatly appreciated. Harold Martin is supported through the NSF Graduate Fellowship Program (GRFP) DGE-1610348.

* Corresponding author.
E-mail address: adjouadi@fiu.edu (M. Adjouadi).

https://doi.org/10.1016/j.bspc.2021.102683
Received 9 February 2021; Received in revised form 4 April 2021; Accepted 24 April 2021
Available online 21 May 2021

support vector machine, a K-nearest neighbor classifier, or an artificial neural network. They also report an intra-patient classifier that utilizes single-lead ECG. Sharma and Sunkaria [8] introduce a 3-lead ECG inferior myocardial infarction classifier for both intra- and inter- patient classification. They used stationary wavelet transforms to produce features later used by k-nearest neighbor or support vector machine classifiers. Liu et al. [9] achieve myocardial infarction classification by using a multiple-feature-branch convolutional neural network on 12-lead electrocardiograms. They present results for intra-patient and a modified version of inter-patient classification where they use the first 32 beats of every patient used for testing during the training phase. Support vector machines are once more used in [10] on 12-lead ECGs to perform intra-patient classification. Support vector machines are also used in [11] along with multiple instance learning. In such study, the authors attempted to detect myocardial infarction from ECG-level topic vectors of a 12-lead ECGs and perhaps develop an intra-patient classifier (as the most likely data split method appears to be file split). In [12] a bagging tree classifier is used to detect myocardial infarctions and arrhythmia. In this study the authors explored which of the ECG's leads would be most appropriate to identify the targeted diseases and arrived at the conclusion that V4 was the most appropriate. However, although good testing metrics are reported, the type of classifier achieved is not quite clear, as the authors did not mention whether they attempted to produce an intra- or inter- patient classifier, nor did they indicate how the data was split into training and testing sets.

Real-time classification of myocardial infarctions is attempted in [13] and [14]. Liu et al. [13] use a multi-lead convolutional neural network to perform the inter-patient classification from a four-lead electrocardiogram. However, they require the whole patient's ECG achieve a diagnosis. Meanwhile, Sopic et al. [14] introduce an event-driven classification technique to be used in wearable systems. They feed a random forest classifier with expert features extracted from a single lead (Lead 5) electrocardiogram to generate an inter-patient diagnosis.

More recently, [15] implemented an algorithm to detect and localize myocardial infarctions from a single beat of 12-lead electrocardiograms. They Dual-Q TQWT along with wavelet packet tensor decomposition and a decision tree to achieve intra-patient classification. In [16], a multi-branch fusion network is implemented and trained on paper ECG to achieve significant detection accuracies and yield an inter-patient classifier. While, finally, [17] trained a multi-lead residual neural network to detect and locate myocardial infarctions from 12-lead ECGs. However, although they set out to create an inter-patient classifier, they end up with something in between intra and inter, as they split their dataset along file lines and not patients, thereby contaminating their test sets.

In our approach, a multilayer Long Short-Term Memory (LSTM) neural network is developed to identify infarcted patients from a single heartbeat of a single-lead (lead II) electrocardiogram. This task is particularly challenging as detecting generalized cases of MI from Lead II alone is challenging because it only focuses on the inferior part of the heart and therefore has a hard time detecting anterior, antero-septal, posterior, and lateral MIs. However, we choose to do so as this lead is extensively available in everyday exercise equipment and fitness trackers, making the deployment of the proposed algorithm feasible and of minimal added cost. Although various types of artificial neural networks have been used in the past to identify myocardial infarctions [6,13,16,17,20–23], we choose to use LSTMs because they have a long and proven track record at classifying time-varying signals such as text, speech, and video [39–46]. Hence, the genesis of their use here to identify heart defects and other cardiac conditions from electrocardiograms. By combining the resulting neural network with an algorithm that detects the R-peaks in real time, the results indicate near-instantaneous detection of myocardial infarctions. Through this expedited diagnosis, this integrated method (LSTM with real-time detection of R peaks) could become extremely beneficial for monitoring patients under cardiac stress and/or at risk of myocardial infarctions while significantly improving the prospects for both the correct diagnosis of the disease condition and for the planning of early treatment.

2. Methods

2.1. Data

The data used in this study was obtained from The Physikalisch-Technische Bundesanstalt (PTB) diagnostic ECG Database [47,48]. This database consists of 549 12-lead individual ECG records collected from 290 subjects (209 men and 81 women) with ages ranging from 17 to 87 years old, of which only 148 myocardial infarction (MI) and 52 Healthy Control (HC) patients are used for this study. However, although 12 leads are available, we only consider Lead II for this study as it is widely used in wearable/portable devices and exercise equipment; thereby positioning the proposed network to be readily deployable in these existing devices and thus eliminating the need to create custom ones. Each record has its associated diagnosis out of which we are interested in the ones containing "acute myocardial infarction", "old myocardial infarction", and "normal control".

A 60 Hz stop-band and a 500-ms moving average filters are applied to remove powerline and low-frequency noise. Once the data is filtered, we apply an Independent Component Analysis (ICA) based algorithm [49] to identify the locations of the ventricular depolarization events (also known as R peaks) and thereafter separate each individual heartbeat to be used in the training phase of the proposed multilayer LSTM network. Each training sample is one second long (500 ms before and 500 ms after the ventricular depolarization event) of the ECG's Lead II data (the information from all other leads within each given record is discarded).

After the data is segmented, it must be separated into groups to be used for training and testing. There are three primary ways in which electrocardiogram heartbeats are separated in the literature when used to detect myocardial infarctions:

Beat-Split: The electrocardiograms in the datasets are split into its constituent heart beats and these are further randomly added to one of the sets (i.e. training, testing, validation, or cross validation sets). In this particular data-split practice we only care that independent heart beats seen during training are not also used for testing. However, individual patients could have a set of heartbeats in the training and another set of heartbeats, albeit different, in the testing set; making it the least restrictive of all methods. This technique is used in the literature to perform **intra-patient** classification [6–10,12,15,24–28,32–34].

File-Split: Also known as Record-Split. As each patient in a given dataset may have multiple recording sessions (record), the individual heart beats associated with each of the individual records can only be present in one of the derived sets. That is, any given record cannot have simultaneous representation in the testing and training sets [15,16,23].

Patient-Split: Each patient (with all of its available records) can only be present in one of the following derived sets (i.e. training, testing, validation, or one of the cross-validation sets). Here, data from patients used for training cannot be used for testing, and vice versa. This technique better ensures that the results achieved during testing will more adequately represent those of new unseen patients. This practice is used in the literature to perform **inter-patient** classification and is the most restrictive data-split method [8,9,13,14,16,33].

As we aim to train a classifier that can be used in real life applications, we use the most restrictive data split available, namely Patient-Split, to ensure that the testing dataset best represents the population at large. As such, once all the independent heart beats have been segmented, each patient (along with all its segmented heartbeats) is assigned to one of 10 distinct and non-overlapping groups, to be used for ten-fold cross-validation. Imperatively, no one patient's data is present in more than one group at any given time. This is important, as having

individual patients simultaneously represented in both the training and testing phases results in overfitting that could yield to misleading high testing metrics, and hence overestimating the performance of the algorithm. Also, this type of data splitting is more amenable to real-world applications, as the network would be trained on a dataset of recorded patient data but will be used and deployed on patients not seen during the training phase.

2.2. Network architecture

We use a three-layer LSTM network to differentiate between subjects with myocardial infarctions (MI) and healthy controls (HC). Layer one and two consist of 100 LSTM units with hyperbolic tangent activations, while the third and last layer is a single LSTM unit with sigmoid activation function. Each training and testing sample is one second long and centered on the ventricular depolarization event (500 ms before and after the R-peak) of the ECG's Lead II data. The design construct of the LSTM model is shown in Fig. 1.

LSTMs, shown in Fig. 2, are a type of recurrent neural networks (RNNs) that see the input signals as time-varying and can therefore make temporal relation inferences about the signals being categorized. Whereas, other common neural networks architectures used in the literature such as convolutional neural networks (CNNs) can only make spatial relations and are therefore limited by the size of their kernels. This is not the case for RNNs as they can learn to remember events indefinitely long in the past of the sequence and make decisions based on it. Also, LSTMs dampen the effect of vanishing gradients present in the original RNNs where events long in the past have diminishing influence in current decisions.

It can be seen from Fig. 2 that an LSTM unit requires as an input its previous state $(s_{(t-1)})$, its last output $(y_{(t-1)})$, and the current input vector (x_t) to generate a new internal state (s_t) and a new output (y_t). Therefore, an LSTM neuron can produce a classification prediction for every input timestep thereby generating time-varying classifications that becomes more accurate and final as more sample points of the signal are processed. This is especially evident in the output activations of the network in Fig. 1, where the final classification label is produced during the last 200 ms of the signal once the PQRST complex has been processed.

This architecture was particularly chosen as it requires no previous expert knowledge of the signal at hand, being able to come up with the features it deems important on its own from the training data. It is also narrower in terms of the required processing steps and hence less complex than other architectures reported in the literature for myocardial infarction classification, making it less prone to overfitting over a limited amount of data as a more complex model gives the network more flexibility to overfit.

The network itself was trained using stochastic gradient decent while implementing L2 regularization [50] with $\lambda = 0.001$, RMSProp updater [51] (learning rate = 0.1, weight decay = 0.95, and epsilon = 10e−6) with weight decay, and gradient clipping (5.0). The weights are initialized using the method proposed by Xavier Glorot [52]. The specific LSTM units used in our study were first described by Alex Graves in [53] to label sequential data such as speech and hand-written text.

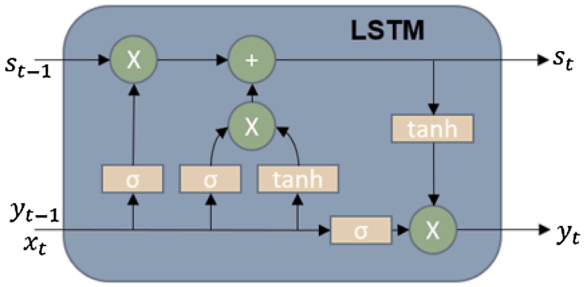

Fig. 2. LSTM unit structure.

The network described herein, was trained and deployed in a 64-bit Windows 10 PC with an AMD FX-8350 Eight-Core Processor, 32 GB of DDR3 RAM, and an NVIDIA GeForce GTX1070. Each training iteration (epoch) took approximately 5 h and covered around 60 K samples, depending on the cross-validation split being used. The network architecture itself was implemented using DeepLearning4J version 0.9.1, a deep learning library for Java.

3. Results and discussion

3.1. Main results

The network is trained using early stopping, for which after 10 epochs of no performance improvement we stop training and back up to the best set of weights. We repeat this process for each of the cross-validation folds. The mean training time is 34.4 epochs (±19.4 epochs 95% CI) when optimizing for accuracy and 27.4 (±12.64 95% CI) epochs when the best J-Measure is the target. The maximum number of epochs required to train any given fold was 75 and the minimum was 4. Classification of a single 1-s sample takes around 40 ms, which would be appropriate for online classification as the time between fast heartbeats is around 300 ms, well above the required processing time.

To measure performance, we have used Accuracy (1), F1-Score (2), Precision (3), Recall (4), Specificity (5), and Youden's J statistic (J-Measure) as defined in (6).

$$\mathrm{Acc} = (\mathrm{TP} + \mathrm{TN})/(\mathrm{TP} + \mathrm{TN} + \mathrm{FP} + \mathrm{FN}) \tag{1}$$

$$F1 = (2 * \mathrm{TP})/(2 * \mathrm{TP} + \mathrm{FP} + \mathrm{FN}) \tag{2}$$

$$\mathrm{Prec} = \mathrm{TP}/(\mathrm{TP} + \mathrm{FP}) \tag{3}$$

$$\mathrm{Recall} = \mathrm{TP}/(\mathrm{TP} + \mathrm{FN}) \tag{4}$$

$$\mathrm{Spec} = \mathrm{TN}/(\mathrm{TN} + \mathrm{FP}) \tag{5}$$

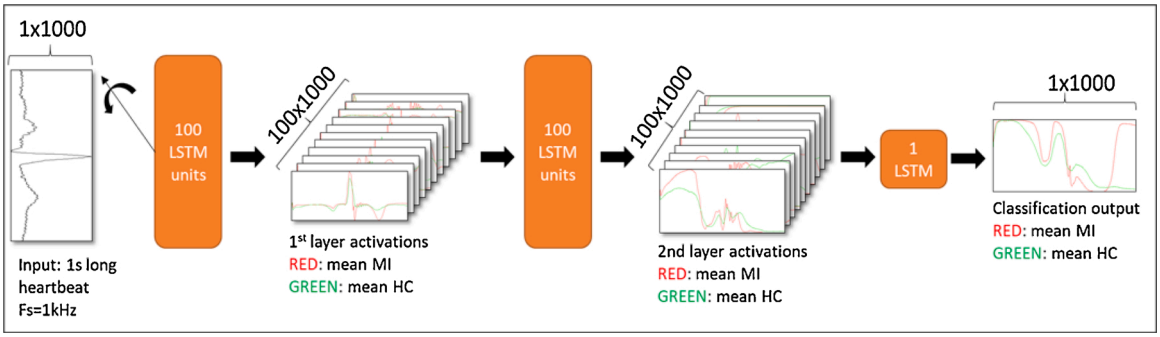

Fig. 1. Network architecture.

$$J = \text{Recall} + \text{Spec} - 1 \quad (6)$$

Where TP stands for true positives, TN for true negatives, FP for false positives, and FN as false negatives.

Table 1 shows the detailed metrics obtained for both optimization methods (accuracy and J measure) on the testing datasets in the 10-fold cross-validation using the Patient-Split approach, and Fig. 3 shows the training progression vs. the testing results of the 80 epochs during the training phase.

It can be observed from these figures that the network starts to stabilize in terms of testing accuracy early in the training, somewhere in between epoch 20 and epoch 25. At that point the network keeps on learning the training dataset, eventually reaching the high nineties before being stopped at epoch 80. This could be due to a lack of significant variability in the training set that would best represent the population at large, a problem which could be addressed by adding more patients into the training dataset.

Another significant fact to appreciate from Table 1 is that the Recall measure is significantly larger than Specificity for either optimizing condition. This is the case mainly because the dataset itself is greatly unbalanced, being largely composed of myocardial infarction patients with significantly less control subjects. To improve performance more controls should be added to the dataset to increase data variability and hence allow the model to better generalize.

3.2. Effects of improper data split

As a retrospective on the performance of various data splits methods and for cautionary measures that should be taken into consideration on the adequacy of data splits, we have trained the proposed model using other state-of-the-art data split methods and show how each can affect the testing results in the way these data splits are performed as detailed in Section 2.

We first focus on the beat-split method (use to generate intra-patient classifiers) and once again use 10-fold cross-validation. However, this time around we only care that independent heart beats seen during training are not also used for testing in accordance with the beat-split method. This nonetheless has a side effect of allowing patients used for training to also be used for testing (since the distinction is made only on the individual heart beats). Fig. 4 shows the training evolution of this particular test case.

These results show that the network's performance on the testing data continuously increases and closely tracks the training metrics. However, the model's performance on new patients should have stabilized early in the training phase, as evidenced from the previous results. Therefore, it is important to review all testing results in combined plots to better understand the model as it is being trained. Fig. 5 shows the testing results for the different types of data splits including beat-split (DB), file-split (DF), and patient-split (DP).

It is evident from these plots that the network first starts to show decreased performance on testing sets that use patient-split followed by test sets generated with file-split. That is, the model seems to start learning to classify the disease but eventually learns something else (perhaps patient level characteristics that help it distinguish hard heartbeats, taking advantage of the lower intra-patient variability). As its performance starts to drop for patients never seen before (as it is the case in DP) and then from files (records) not seen during training (DF) it appears to learn features that are shared across files and eventually features shared across heart beats of the same patient; effectively memorizing patients by learning to identify which beats belong to patients seen during training and assigning them the appropriate diagnosis based on prior knowledge.

It is also important to point out that minor epoch-level differences among the three split modes (DB,DF, and DP) are due to the nature of training; where the classifier focuses on different features at different timepoints as it descends down the multidimensional gradient in its attempt to minimize the classification error. What should be taken from the plots is the general direction/trend of the plotlines themselves and not the local differences.

3.3. Randomizing labels of myocardial infarction patients and healthy controls

Because the network could be learning many things, and not specifically memorizing patients, we take it one step further and randomize the labels (MI/Controls) of each patient before retraining the model using beat-split. This action effectively eliminates any existing link(s) between biomarkers and disease label. Therefore, if the network model was never about memorizing the patients but just about learning the nature of the disease, we would not be able to attain a mean accuracy greater than 50%, given that the new labels are uniformly and randomly distributed.

This time around, we trained the network for 90 epochs to identify any distinctive patterns that may arise. Fig. 6 shows the results of the experiment.

These results clearly show that the proposed network is capable of learning features that help it identify heart beats from previously seen patients, effectively memorizing them, if adequate time is given. Therefore, it is of paramount importance that an adequate data-splitting method be used when creating the training and testing datasets, as choosing an inappropriate one will mask overfitting and lead to erroneously high testing metrics that are not representative of the model's performance on the general population.

3.4. Influence of MI location on detection rate

The location of the myocardial infarction has a great potential to influence the detection rate of the proposed classifier. As we choose to use a single ECG lead, the model proposed herein has a limited view of the heart's electrical activity and certain MI types could be obscured from such a view.

In practice, we can encounter various types of MIs which themselves affect the electrical activity of different sections of the heart. In the database used for this study, there are four main types of infarction that are described as follows:

Anterior MIs happen when the left anterior descending (LAD) coronary artery is obstructed, which could lead to changes in leads V1 through V6 but might or might not show in Lead II, depending on where the occlusion happens. *Antero-Lateral* MIs (a combination of Anterior and Lateral) show up in leads V3 through V6, while *Antero-Septal* MIs can be seen in leads V1 through V4. All along, these types of Anterior MIs could produce changes in Lead II depending on the location of the LAD occlusion [54].

Inferior MIs, account for about 40% of all MIs and generally involve a blockage of the right coronary artery. When the Inferior region is the main location of the infarction, leads II, III, aVF, and aVL show changes

Table 1
Testing results of the proposed LSTM method.

Optimization	Acc	F1	Prec	Recall	Spec	J	# Epochs
Acc	91.36 (±2.88%)	94.71 (±1.97%)	93.54 (±2.46%)	96.00 (±2.45%)	69.28 (±8.41%)	65.28 (±8.41%)	34.40 (±19.40)
J	89.56 (±2.79%)	93.45 (±1.94%)	95.30 (±2.86%)	91.88 (±3.13%)	80.81 (±9.62%)	72.69 (±8.98%)	27.40 (±12.64)

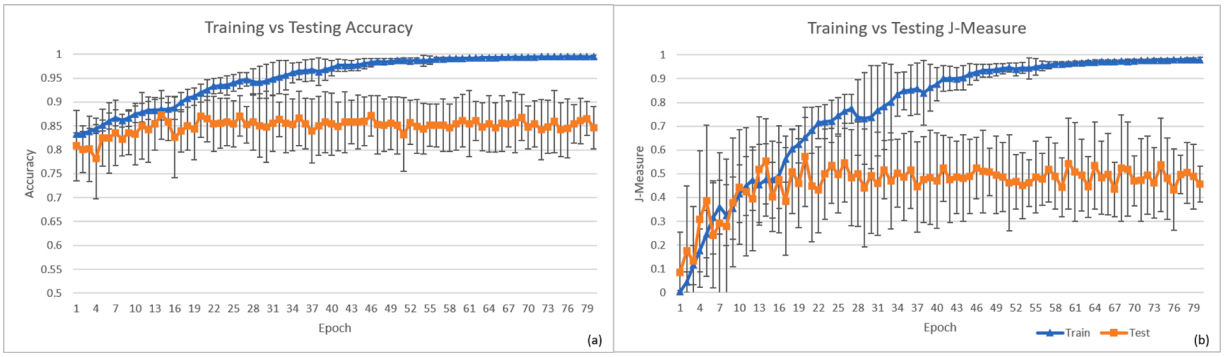

Fig. 3. Evolution of performance metrics for the training and testing phase for the proposed LSTM model. (a) Accuracy, (b) J-Measure.

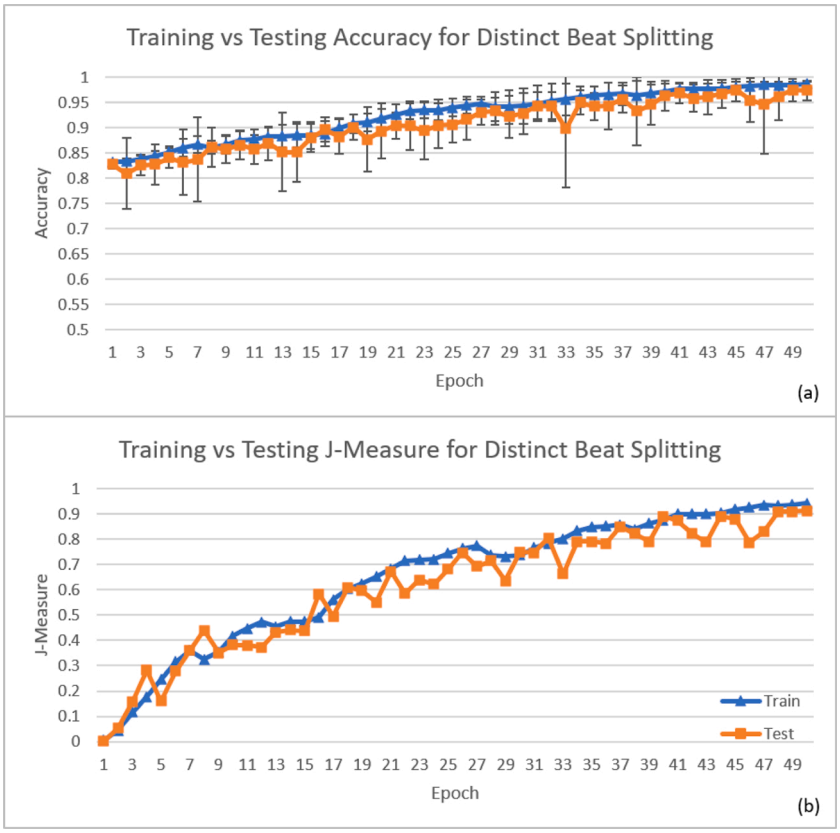

Fig. 4. Evolution of performance metrics of the beat splitting method for both the training and testing phase. (a) Accuracy, (b) J-Measure.

in their respective electrical activity [55].

Lateral MIs are rare in their pure form; they generally occur as part of larger infarctions involving multiple areas, because the left ventricular lateral wall is perfused by the left anterior descending artery and the left circumflex artery. Leads I, III, aVL, aVF, V5, and V6 can all show electrical changes associated with Lateral MIs [56].

Posterior MIs present subtle changes in ECGs, therefore making them challenging to diagnose when they occur in isolation and often lead to misdiagnosis. They commonly take place in combination with Inferior and Infero-Lateral MIs. Purely posterior MIs can be hard to observe in ECGs and might require the addition of extra leads not present in the typical 12-lead ECGs (V7-V9) [57].

Fig. 7 shows the detection rates of the proposed MI detector according to the location of the myocardial infarction as well as the availability of samples for each of the cases.

It is evident from this figure that the cases where the model underperforms (*Lateral* and *Posterior*) are ones where the electrical changes associated with them are hard to observe from the lead used in this study [56,57]. On the other hand, we must also be cautious of cases where the model performs exceedingly well, especially *Antero-Septo-Lateral* and *Infero-Posterior*, as the number of available samples for training and testing is minuscule.

3.5. Behavior when encountering other pathologies

Although various pathologies are present in the PTB database, we only used the data available form patients diagnosed with myocardial infarctions and that from healthy controls for both training and testing. However, much like in real life, the proposed model will encounter samples from classes other than MI or HC. Therefore, we would benefit from understanding or at least viewing how the classifier would respond when presented with samples from these other classes.

In this section, we run all samples from every patient from the PTB not used in this study through the already trained classifiers for each fold

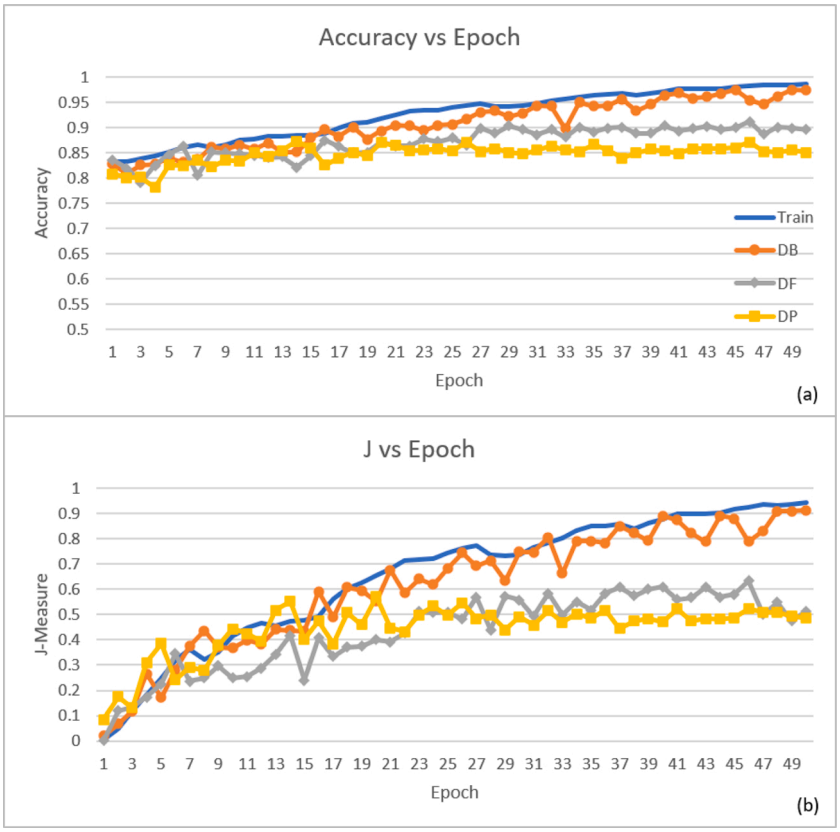

Fig. 5. Evolution of performance metrics for the different data split methods. (a) Accuracy, (b) J-Measure. *DB->Beat-Split; DF → File-Split; DP → Patient-Split.

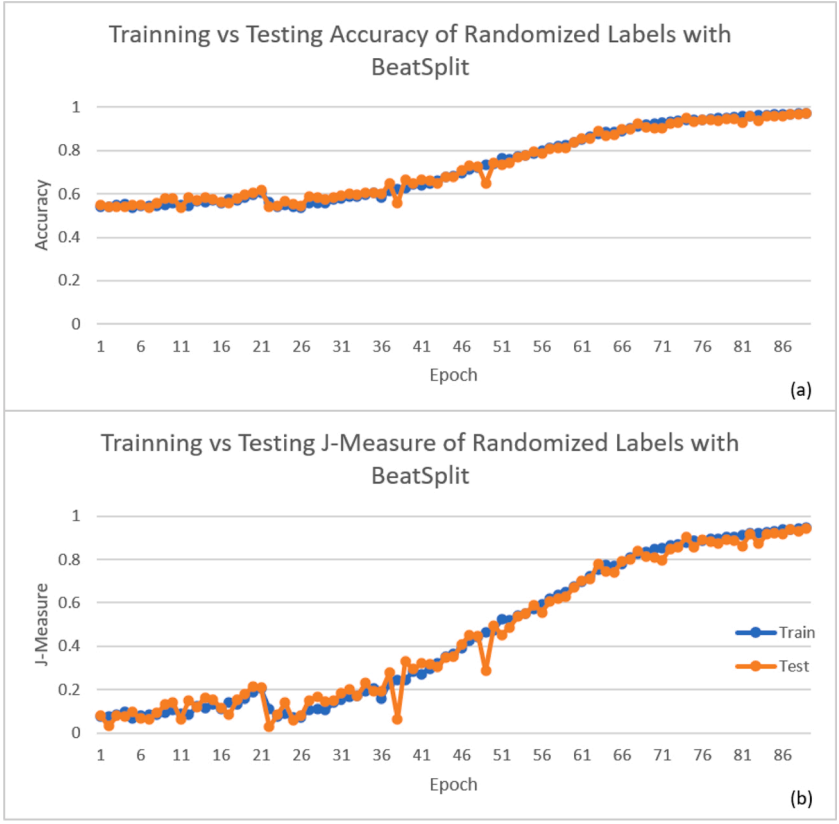

Fig. 6. Evolution of performance metrics for randomized labels datasets. (a) Accuracy, (b) J-Measure.

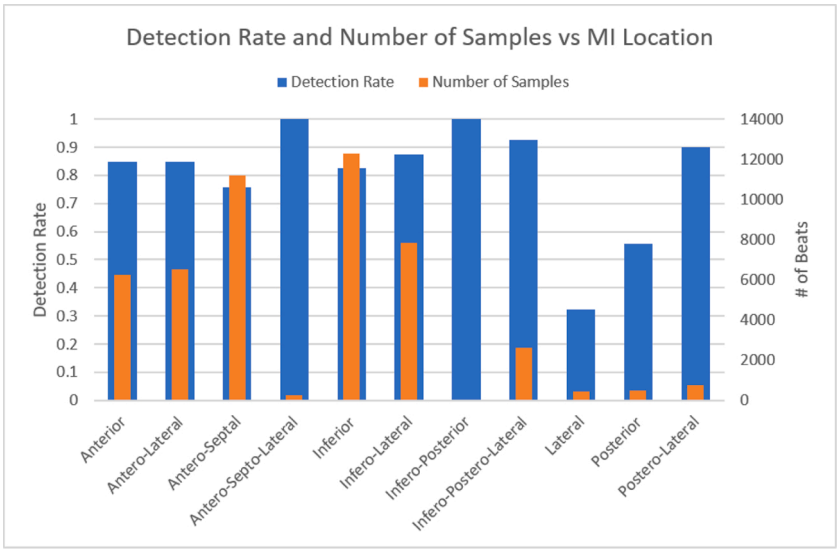

Fig. 7. Detection rate according to MI location.

of training and report the average detection rate along with the respective standard deviation.

Fig. 8 shows the distribution of the classifier's output for heartbeats from patients with a main diagnosis other than myocardial infarction or healthy control. In this figure the columns are associated with a given reason for admission and each of them has two colors; orange represents MI and blue represents HC. If a column is mostly composed of orange that means that most of the heartbeats associated with that diagnosis are classified as MI by the proposed model, while if mostly blue is present the classifier saw them as HCs.

In this figure, we can see the primary reasons for admission present in the PTB header files associated with each record. Going even deeper, we can further break down how within each reason for admission the classifier proposed herein treats each subject.

Bundle Branch Block: There are 20 independent records, belonging to 18 different patients, that list bundle branch block as a diagnosis. Of them, 17 (from 15 different patients), this condition was listed as the reason for the ECG and admission to the hospital and only 5 records (from 4 distinct patients) had more than fifty percent (50%) of its heartbeats classified as healthy controls.

Cardiomyopathy: There are 17 independent records (from 15 different patients) for which this condition was listed as the reason for the ECG and admission to the hospital. Of these only 2 records had more than fifty percent (50%) of its heartbeats classified as healthy controls and they each belonged to different patients.

Dysrhythmia: There are 16 different files from 14 different patients for which the main reason for admission was the condition of dysrhythmia. However, dysrhythmia condition rarely appeared alone and "Atrial Fibrillation" (AFib) was also evident in 8 (50%) of them where more than fifty percent (50%) of the heartbeats in each of those records were classified as belonging to the myocardial infarction class. "Coronary Artery Disease" (CAD) also accompanied dysrhythmia. Only one record from a single patient containing the main diagnosis of dysrhythmia had more than fifty percent (50%) of its heartbeats classified as healthy controls.

Heart Failure (Types 2,3, and 4): There are very limited number of records exhibiting heart failure; only one of each type from separate subjects exist in the PTB. Each of this records had a very high percentage ($>$ 96%) of its constituent heartbeats classified as MI.

Hypertrophy: is present as the main reason for admission in seven (7) ECGs from seven patients. Hypertrophy was never diagnosed alone and only one patient's record (being additionally diagnosed with hypertension) had 93% of its heartbeats classified as healthy. For all other records, at least 61% of the heartbeats where considered infracted.

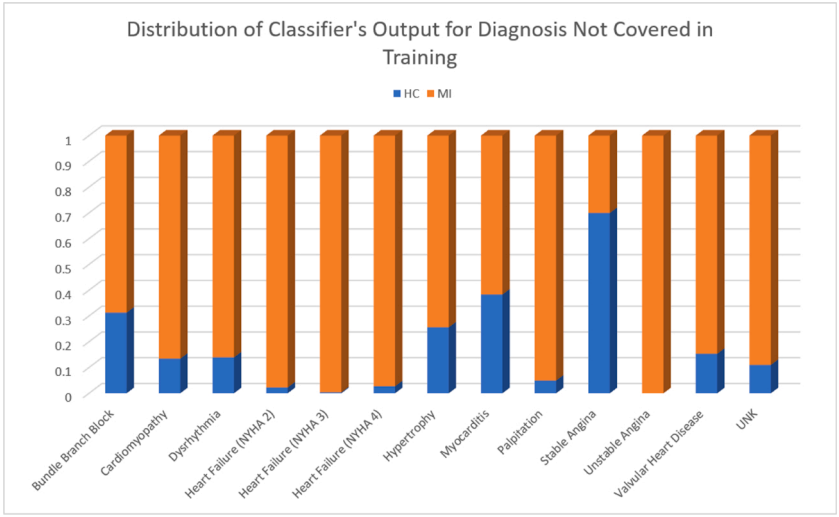

Fig. 8. Distribution of classifier's output for diagnosis not covered in training.

Myocarditis: is observed in four (4) records form four (4) distinct patients. Only one of these records had most (> 94%) of its heartbeats classified as healthy. The record with most beats classified as MI (> 84%) has an additional diagnosis of "Bundle Branch Block".

Palpitation: are only present in one single record where over 95% of the heartbeats are classified as infarcted. This record also had an additional diagnosis of Coronary Heart Disease.

Stable Angina: is the main reason for the admission of two separate patients (for a total of two ECGs). One of them only has additional cold and Hyperlipoproteinemia as a diagnosis and received a healthy classification for over 90% of its heartbeats. The other has CAD and hypertension, resulting in over 95% of its heartbeats being classified as MI.

Unstable Angina: is only present in one record and 100% of the beats are classified as MI.

Valvular heart disease: is listed as the main reason for the admission of six (6) patients, for a total of six (6) ECGs. Every one of these records has multiple associated diagnoses and over 75% of the heartbeats in each record were classified as MI.

Atrial Fibrillation (AFib): is never listed as the main reason for the admission of any patient but is listed as an associated diagnosis in fourteen (14) separate records from eleven (11) patients. Every time AFib is listed as a diagnosis for a given record, over 60% of the heartbeats therein were classified as MI.

Unknown (UNK): The reason for the admission of 22 patients is listed as unknown. From these, 27 separate records were recorded. Most of them have over 90% of their heartbeats classified as MIs, about 22 records. Of the remaining five (5), four (4) have over 50% of the heartbeats classified as MI and only one has over 90% of them classified as healthy.

It seems to be evident from these broad statistics that the model proposed in this study, although only trained to differentiate between myocardial infarctions and healthy controls, appears to be detecting life threatening heart ailments. This possibility would have to be further explored in future studies that encompass broader datasets, as no conclusive finding can be done over these limited samples.

3.6. Visualizing the errors

Although high classification metrics were achieved using the proposed approach, it is important to understand where the proposed model falls short and does not achieve the best performance. To start, Fig. 9 depicts interestingly different heartbeats from specific records were the classification accuracy was particularly low (<10%).

The heartbeat present in Fig. 9a belongs to a patient originally admitted for an *Anterior MI* but the ECG was recorded over a year after the infarction took place, to be more specific 396 days after. This heartbeat was classified by the model as "Healthy Control" although the truth value from the diagnosis was "Myocardial Infarction" making it a false negative. Only eleven (11) out of the one-hundred and forty-two (142) heartbeats for patient 120 were correctly labeled as MI instead of HC.

Fig. 9b shows an example of improper lead placement or contact that yielded a very noisy ECG recording. This heartbeat belongs to patient 180, a healthy control subject, and is part of record s0476_re. In this record, there is a vast amount of noise present in Lead II, while leads 1 through 6 are fairly clean. However, as this classifier only uses the information from Lead II it is hindered by the noise and is challenged to properly classify the detected heartbeats. Only one (1) out of the two-hundred and forty-one (241) detected heartbeats is properly classified as HC, while all others are improperly labeled as MI.

A truly interesting false positive case is present in Fig. 9c. This heartbeat also belongs to patient 180, but this time the record is s0561_re and there is no significant noise to contend with. In this instance, the classifier was unable to properly classify around 63% of all detected heartbeats, assigning them an MI label instead of the correct HC.

Fig. 9d shows another instance of a false negative outcome. This heartbeat belongs to records s0141lr of patient 43, a subject with a lateral infarction. In this instance there are a couple of factors that made the classification difficult: (1) the electrocardiogram was recorded over eight (8) months after the infarction took place and a catheterization was performed, and (2) the type of infarction in question was a "Lateral MI", which are difficult to diagnose from Lead II alone as electrical activity changes associated with it might not be revealed in such a lead [56].

3.7. Comparative assessment

As the type of data split used for training is seen to greatly affect the performance metrics, we must restrict our comparative assessment contrasting the proposed method to related studies that use the same data split method in order to avoid unfair comparisons. Some relevant studies covered in the literature are presented in Table 2. Herein, we provide a simplified evaluation of their dataset generation techniques

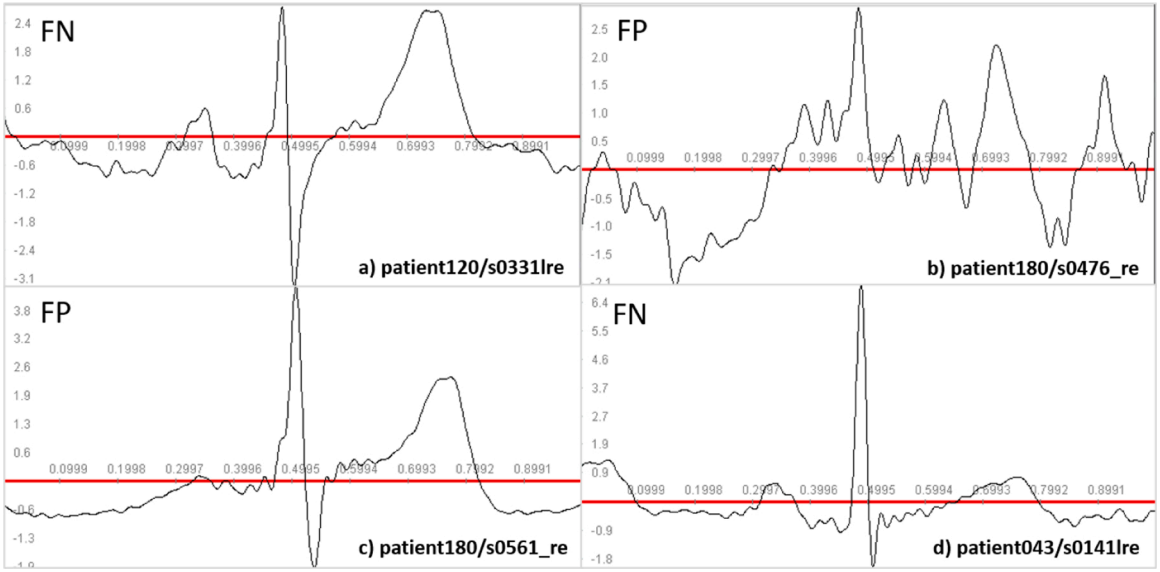

Fig. 9. Examples of misclassified heartbeats.

Table 2
Simplified analysis of relevant studies.

Study	# Leads	Sample Length	Beat Split	File Split	Patient Split
[6]	1	0.65 s	×		
[7]	1	RR interval	×		
[8]	3	3 s	×		×
[9]	12	1 s	×		×
[10]	12	10 s	×		
[12]	1	2 beats	×		
[13]	4	Whole record			×
[14]	1	0.65 s			×
[15]	12	0.65 s	×	×	
[16]	12	7 s		×	×
[17]	12	4 s		×	

along with the number of leads used and the sample size required to make a classification.

Given the unique way of assuming only a single heart beat and single-lead electrocardiograms together with the adoption of patient split method of analyzing data, to the best of our knowledge, there are no other studies of myocardial infarction detection and classification that can be completely and fairly compared to ours, as types of MI classified vary and the datasets and dataset subsets are not equal to ours. However, in Table 3 we provide an in depth comparison of some of the available studies that generate inter-patient detection of MI. In this table, we cover and provide the numbers of leads used, number of patients and heartbeats evaluate, the sample length required, the method used, and the general performance metrics of each study.

Of all the studies presented herein, [8] and [14] are somewhat close, although much more restrictive (they use subsets of the available data), as they use electrocardiograms available from the PTB diagnostic ECG Database [47,48].

Sharma and Sunkaria [8] focused on acute myocardial infarctions in the inferior portion of the heart (IMI) leading them to a rather restricted dataset of only 30 MI subjects and 52 HC. Moreover, they use three leads of the available twelve, specifically leads II, III and aVF, as better representatives of electrical activity in the inferior portion of the heart. Sopic et al. [14] use random forest feed by expert features extracted from Lead 5 of the available electrocardiograms using discrete wavelet transforms. They use 52 MI subjects as they want to keep a balanced set for training and testing due to the limited availability of healthy controls (52). Just as in [8], this study is not directly comparable to ours as they use a different ECG lead and a more restrictive, yet balanced dataset.

Although our results are not directly comparable, we achieve the highest accuracy and recall, when comparing against either [8] or [14], for either of the two optimization cases (best Accuracy or best balance between Specificity and Recall). However, our specificity and J-Measure oscillate, providing the best number only when we train our network to achieve the best balance between Specificity and Recall. The lower specificity is likely due to the fact that we have a heavily unbalanced dataset, as there are about three times more myocardial infarction subjects than healthy controls in our datasets, and a higher accuracy will tend to lead the network to prioritize properly classifying MI records over HCs. We overcome this in this study, by optimizing, or targeting the point in time at which the network is having the best balance between specificity and recall instead of using the common practice of just targeting the best accuracy. We also only require one lead of the electrocardiogram as does [14] but unlike them our lead is more commonly sampled and simpler to record that lead V5. Neither [8] nor [14] provides the diagnosis time (or processing time), but study [14] provides a hardware implementation which is commendable and could be used as means to reduce the processing time.

From Table 3 we can also see that the detection accuracy is positively correlated with the number of leads used, that is, more leads equals greater accuracy. This is to be expected, as more electrocardiogram's leads equates to more views of the heart and more information is gathered. The extra information collected from other leads is especially useful to detect infarctions that are not visible or hard to see from a single lead, as it is our case [56,54,57]. By using 12-lead ECGs, [9] and [16] are able to achieve higher performance metrics than any other single lead method.

Longer sample lengths seem to also influence the performance of the different models, but the relevance of this pattern is not very clear. In the case of [13], by using the whole record to produce a classification, the authors achieve higher performance metrics than those reported by [16] who used more leads (12 in [16] vs. 4 in [13]). However, [16] is detecting MI from ECG images, not digital signals like all other studies in Table 3 are, and this could explain the difference in performance. The authors of [13] also tailored their lead selection to the type of MI they were trying to detect (Generalized Anterior MI) which makes it less clear whether or not the sample length is the key factor yielding the performance improvement. Therefore, it is hard to gauge the influence of sample length in classifier performance due to the fact that such vary from study to study along with classification method, number of leads, and even dataset used. To the best of our knowledge there is no study that explores the influence of sample length on MI detection rate.

One more significant factor to point out is that we are not able to provide a statistical comparison of our method to other present in the literature or those presented in this section, as they only provide the average performance metrics of their validation approaches and do not provide the standard deviations of such.

Overall, the results obtained are highly competitive in comparison to state-of-the-art algorithms, although stringent conditions are set up in the training phase to overcome overfitting, data leakage and bias from

Table 3
Comparative results of methods using patient split method.

Study	Leads used	#Patients	# Beats	Sample length	Method	Acc	Recall	Specificity	J-Measure
[8]	II, III, aVF	30MI, 52HC	3240 MI, 3037 HC	3 s	SWT &SVM	81.71	79.01	79.26	58.27
[9]	12	128MI, 52HC	48690MI, 10646HC	1 s	MFB-CNN	98.79	98.73	99.35	98.08
[13]	aVL,V2, V3,V5	Records: 167MI, 80HC	Not Specified	Whole Record	ML-CNN	96.00	95.40	97.37	92.77
[14]	V5	52MI, 52HC	Not Specified	0.65 s	Random Forest	83.26	87.95	78.82	66.77
[16]	12	Images: 483MI, 474HC	Not Specified	7 s	MBFN-CNN	94.73	96.41	95.94	92.35
Proposed (Accuracy Optimization)	II	148MI, 52HC	50732MI, 10123HC	1 s	LSTM	91.36 (±2.88%)	96.00 (±2.45%)	69.28 (±8.41%)	65.28 (±8.41%)
Proposed (J-Measure Optimization)	II	148MI, 52HC	50732MI, 10123HC	1 s	LSTM	89.56 (±2.79%)	91.88 (±3.13%)	80.81 (±9.62%)	72.69 (±8.98%)

features seen in the training phase. The proposed method would have performed even better if a balance between the normal controls and MI subjects could have been reached through the collection of more data from normal controls.

4. Conclusion

We propose a novel multilayer LSTM neural network for near-real time and accurate infarction detection using one-second ECG samples of Lead II ECGs. This study considered 148 myocardial infarction patients and 52 healthy controls which were split into 10 non-patient-overlapping sets for 10-fold cross validation. The proposed algorithm, which uniquely relies on a single heartbeat of single-lead (lead II) electrocardiograms, achieved an accuracy of 89.56% (with a 95% Confidence Interval of ±2.79%), recall/sensitivity of 91.88% (±3.13% 95%CI), and a specificity of 80.81% (±9.62% 95%CI). It is important to emphasize that in the approach considered, while deploying the patient split method, care was taken that no heart beats or subjects (MIs and HCs) seen in the training phase are considered in the testing phase. Moreover, within the design construct of the model, we aimed to achieve near real-time infarction detection yielding a processing time of only 40 ms to diagnosis, which is well within the time in between two heartbeats of 300 ms assuming a fast heart rate. This fast-processing characteristic of the model allows for its deployment on existing wearable/portable devices and other test instruments which could potentially have significant societal and clinical impact in the lives of not only at-risk patients but also for the population at large.

However, the immediate impact of accurately providing a real-time infarction diagnosis would largely depend on the number of at-risk patients. A portion of myocardial infarction mortality rate is due to the lack of immediate medical assistance resulting from lack of awareness and/or absence of observable symptoms. By monitoring the ECG of patients under cardiac stress and/or at risk of myocardial infarctions in near real-time, we could speed up the time to diagnosis, plan for early treatment, and extend the window of time for doctors to tackle the problem in case of an emergency.

Furthermore, integrating the proposed approach to a standalone software/hardware platform that would monitor a patient's cardiac activity, perhaps through the use of widely available fitness trackers and other currently commercially available wearable devices, would be a significant portion of our research efforts for the next step in the development of this software-based design. Moreover, given the implemented architecture of this LSTM model, we could also seek to identify at which point of the heartbeat the presence of myocardial infarctions becomes evident, as the last LSTM layer can be set up to provide a per-timestep diagnosis.

Credit author statement

Harold Martin: Conceptualization, Data Curation, Formal Analysis, Investigation, Methodology, Software, Validation, Visualization, Original Draft. **Walter Izquierdo**: Conceptualization, Data Curation, Formal Analysis, Investigation, Methodology, Validation. **Mercedes Cabrerizo**: Conceptualization, Investigation, Methodology, Resources, Supervision, Validation, Review and Editing. **Anastasio Cabrera**: Investigation, Methodology, Supervision, Validation, Review and Editing. **Malek Adjouadi**: Conceptualization, Investigation, Methodology, Funding Acquisition, Project Administration, Resources, Supervision, Review and Editing.

Declaration of Competing Interest

The authors declare that they have no known competing financial interests or personal relationships that could have appeared to influence the work reported in this paper

References

[1] "Heart Attack" Aug. 18,2017. Available from: https://www.cdc.gov/heartdisease/heart_attack.htm [Online].
[2] "Heart Disease Fact Sheet" Aug. 23, 2017. Available from: https://www.cdc.gov/dhdsp/data_statistics/fact_sheets/fs_heart_disease.htm [Online].
[3] G. Nicholson, S.R. Gandra, R.J. Halbert, A. Richhariya, R.J. Nordyke, Patient-level costs of major cardiovascular conditions: a review of the international literature, ClinicoEcon. Outcomes Res. 8 (September) (2016) 495–506.
[4] R. Barnett, Case histories acute myocardial infarction, Lancet 393 (June (10191)) (2019) 2580.
[5] P. Kligfield, L.S. Gettes, J.J. Bailey, R. Childers, B.J. Deal, E.W. Hancock, G. van Herpen, J.A. Kors, P. Macfarlane, D.M. Mirvis, O. Pahlm, P. Rautaharju, G. S. Wagner, Recommendations for the standardization and interpretation of the electrocardiogram – Part I, Circulation 25 (March (10)) (2007) 1306–1324.
[6] U.R. Acharya, H. Fujita, S.L. Oh, Y. Hagiwara, J.H. Tan, M. Adam, Application of deep convolutional neural network for automated detection of myocardial infarction using ECG signals, Inf. Sci. 415 (November) (2017) 190–198.
[7] P. Kora, ECG based myocardial infarction detection using hybrid firefly algorithm, Comput. Methods Programs Biomed. 152 (December) (2017) 141–148.
[8] L.D. Sharma, R.K. Sunkaria, Inferior myocardial infarction detection using stationary wavelet transform and machine learning approach, Signal Image Video Process. 12 (February (2)) (2018) 199–206.
[9] W. Liu, Q. Huang, S. Chang, H. Wang, J. He, Multiple-fracture-branch convolutional neural network for myocardial infarction diagnosis using electrocardiogram, Biomed. Signal Process. Control (2018).
[10] A.K. Dohare, V. Kumar, R. Kumar, Detection of myocardial infarction in 12 lead ECG using support vector machine, Appl. Soft Comput. 64 (March) (2018) 138–147.
[11] L. Sun, Y. Lu, K. Yang, S. Li, ECG analysis using multiple instance learning for myocardial infarction detection, IEEE Trans. Biomed. Eng. 59 (December (12)) (2010) 3348–3356.
[12] S. Khatun, B.I. Morshed, Detection of myocardial infarction and arrhythmia from single-lead ECG data using bagging trees classifier, in: IEEE International Conf. on Electro Information Technology (EIT), May 14–17, 2017.
[13] W. Liu, M. Zhang, Y. Zhang, Y. Liao, Q. Huang, S. Chang, H. Wang, J. He, Real-time multilead convolutional neural network for myocardial infarction detection, IEEE J. Biomed. Health Inform. 22 (September (5)) (2018) 1434–1444.
[14] D. Sopic, A. Aminifar, D. Atienza, Real-time event-driven classification technique for early detection and prevention of myocardial infarction on wearable systems, IEEE Trans. Biomed. Circuits Syst. 12 (October (5)) (2018) 982–992.
[15] J. Liu, C. Zhang, Y. Zhu, T. Ristaniemi, T. Parviainen, F. Cong, Automated detection and localization system of myocardial infarction in single-beat ECG using Dual-Q TQWT and wavelet packet tensor decomposition, Comput. Methods Programs Biomed. 184 (February) (2020) 105120.
[16] P. Hao, X. Gao, Z. Li, J. Zhang, F. Wu, C. Bai, Multi-branch fusion network for myocardial infarction screening from 12-lead ECG images, Comput. Methods Programs Biomed. 184 (February) (2020) 105286.
[17] C. Han, L. Shi, ML-ResNet: a novel network to detect and locate myocardial infarction using 12 leads ECG, Comput. Methods Programs Biomed. 185 (March) (2020) 105138.
[18] D. Sadhukhan, S. Pal, M. Mitra, Automated identification of myocardial infarction using harmonic phase distribution pattern of ECG data, IEEE Trans. Instrum. Meas. 67 (October (10)) (2018) 2303–2313.
[19] S. Padhy, S. Dandapat, Third-order tensor based analysis of multilead ECG for classification of myocardial infarction, Biomed. Signal Process. Control 31 (July) (2016) 71–78.
[20] W.G. Baxt, Application of artificial neural networks to clinical medicine, Lancet 346 (October (8983)) (1995) 1135–1138.
[21] W.G. Baxt, J. Skora, Prospective validation of artificial neural network trained to identify acute myocardial infarction, Lancet 347 (January (8993)) (1996) 12–15.
[22] W.G. Baxt, F.S. Shofer, F.D. Sites, J.E. Hollander, A neural computational aid to the diagnosis of acute myocardial infarction, Ann. Emerg. Med. 39 (April (4)) (2002) 366–373.
[23] B. Heden, H. Ohlin, R. Rittner, L. Edenbrandt, Acute myocardial infarction detected in the 12-lead ECG by artificial neural networks, Circulation 96 (September (6)) (1997) 1798–1802.
[24] L.N. Sharma, R.K. Tripathy, S. Dandapat, Multiscale energy and eigenspace approach to detection and localization of myocardial infarction, IEEE Trans. Biomed. Eng. 62 (July (7)) (2015) 1827–1837.
[25] P. Li, Y. Wang, J. He, L. Wang, Y. Tian, T.S. Zhou, T. Li, J.S. Li, High-performance personalized heartbeat classification model for long-term ECG signal, IEEE Trans. Biomed. Eng. 64 (January (1)) (2017) 78–86.
[26] U.R. Acharya, H. Fujita, V.K. Sudarshan, S.L. Oh, M. Adam, J.E.W. Koh, J.H. Tann, D.N. Ghista, R.J. Martis, C.K. Chua, C.K. Poo, R.S. Tan, Automated detection and localization of myocardial infarction using electrocardiogram: a comparative study of different leads, Knowl.-Based Syst. 99 (May) (2016) 146–156.
[27] U.R. Acharya, H. Fujita, V.K. Sudarshan, S.L. Oh, M. Adam, J.H. Tann, J.H. Koo, A. Jain, C.M. Lim, K.C. Chua, Automated characterization of coronary artery disease, myocardial infarction, and congestive heart failure using contourlet and shearlet transforms of electrocardiogram signal, Knowl.-Based Syst. 132 (September) (2017) 156–166.
[28] H. He, Y. Tan, J. Xing, Unsupervised classification of 12-lead ECG signals using wavelet tensor decomposition and two-dimensional Gaussian spectral clustering, Knowl.-Based Syst. 163 (January) (2019) 392–403.

[29] P. Gomis, D.L. Jones, P. Caminal, E.J. Berbari, P. Lander, Analysis of abnormal signals within the QRS complex of the high-resolution electrocardiogram, IEEE Trans. Biomed. Eng. 44 (August (8)) (1997) 681–693.
[30] A. Spiegl, P. Steinbigler, I. Schmucking, A. Knez, R. Haberl, Analysis of beat-to-beat variability of frequency contents in the electrocardiogram using two-dimensional Fourier transforms, IEEE Trans. Biomed. Eng. 45 (February (2)) (1998) 235–241.
[31] M.M. Ghiasi, S. Zendehboudi, A.A. Mohsenipour, Decision tree-based diagnosis of coronary artery disease: CART model, Comput. Methods Programs Biomed. 192 (August) (2020) 105400.
[32] M. Sharma, R.S. Tan, U.R. Acharya, A novel automated diagnosis system for classification of myocardial infarction ECG signals using an optimal biorthogonal filter bank, Comput. Biol. Med. 102 (2018) 341–356.
[33] J.H. Tan, Y. Hagiwara, W. Pang, I. Lim, S.L. Oh, M. Adam, R.S. Tan, M. Chen, U. R. Acharya, Applications of stacked convolutional and long short-term memory network for accurate identification of CAD ECG signals, Comput. Biol. Med. 94 (2018) 19–26.
[34] B. Liu, J. Liu, G. Wang, K. Huang, F. Li, Y. Zheng, Y. Luo, F. Zhou, A novel electrocardiogram parametrization algorithm and its application in myocardial infarction detection, Comput. Biol. Med. 61 (2015) 178–184.
[35] L. Yao, P. Li, C. Liu, Y. Hou, C. Yan, L. Li, K. Li, X. Wang, A. Deogire, C. Du, H. Zhang, J. Wang, H. Li, Comparizon of QT interval variability of coronary patients without myocardial infarction with that of patietns with old myocardial infarction, Comput. Biol. Med. 113 (2019) 103396.
[36] R. Alizadehsani, M. Abdar, M. Roshanzamir, A. Khosravi, P.M. Kebria, F. Khozeimeh, S. Nahavandi, N. Sarrafzadegan, U.R. Acharya, Machine learning-based coronary artery disease diagnosis: a comprehensive review, Comput. Biol. Med. 111 (2019) 103346.
[37] K. Jafarian, V. Vahdat, S. Salehi, M. Mobin, Automating detection and localization of myocardial infarction using shallow and end-to-end deep neural networks, Appl. Soft Comput. 93 (2020).
[38] M. Wasimuddin, K. Elleithy, A. Abuzneid, M. Faezipour, O. Abuzaghleh, Stages-based ECG signal analysis from traditional signal processing to machine learning approaches: a survey, IEEE Access (2020).
[39] H.G. Zen, H. Sak, Unidirectional long short-term memory recurrent neural network with recurrent output layer for low-latency speech synthesis, in: 2015 IEEE International Conference On Acoustics, Speech, And Signal Processing (ICASSP), 19–24 April, Brisbane, Australia, 2015.
[40] T.M. Breuel, A. Ul-Hasan, M. Azawi, F. Shafait, High-performance OCR for printed English and Fraktur using LSTM networks, in: 12th International Conference on Document Analysis And Recognition (ICDAR), 25–28 August, Washington DC, 2013.
[41] A. Ullah, J. Ahmad, K. Muhammad, M. Sajjad, S.W. Baik, Action recognition in video sequences using deep bi-directional LSTM with CNN features, IEEE Access 6 (2018) 1155–1166.
[42] D.L. Marino, K. Amarasinghe, M. Manic, Building energy load forecasting using deep neural networks, in: 42nd Annual Conference of The IEEE Industrial Electronics Society, 24–27 October, Florence, Italy, 2016.
[43] K. Zhang, J.W. Xu, M.R. Min, G.F. Jiang, K. Pelechrinis, Automated IT system failure prediction: a deep learning approach, in: 4th IEEE International Conference on Big Data, 5–8 December, Washington, DC, 2016.
[44] M.R. Yousefi, M.R. Soheili, T.M. Breuel, E. Kabir, D. Stricker, Binarization-free OCR for historical documents using LSTM networks, in: 13th IAPR International Conference on Document Analysis And Recognition (ICDAR), 23–26 August, Nancy, France, 2015.
[45] Y. Luo, Recurrent neural networks for classifying relations in clinical notes, J. Biomed. Inform. 72 (August) (2017) 85–95.
[46] Q.C. Zhang, L.T. Yang, Z.K. Chen, P. Li, A survey on deep learning for big data, Inf. Fusion 42 (July) (2018) 146–157.
[47] R. Bousseljot, D. Kreiseler, A. Schnabel, "Nutzung der EKG-Signaldatenbank" CARDIODAT der PTB über das Internet. Biomedizinische Technik, Band 40, Ergänzungsband 1 (1995) S 317.
[48] A.L. Goldberger, L.A.N. Amaral, L. Glass, J.M. Hausdorff, P.C. Ivanov, R.G. Mark, J. E. Mietus, G.B. Moody, C.-K. Peng, H.E. Stanley, PhysioBank, PhysioToolkit, and PhysioNet: components of a new research resource for complex physiologic signals, Circulation 101 (June (23)) (2000) e215–e220 [Circulation Electronic Pages; http://circ.ahajournals.org/content/101/23/e215.full].
[49] H. Martin, W. Izquierdo, M. Cabrerizo, M. Adjouadi, Real-time R-spike detection in the cardiac waveform through independent component analysis, in: 2017 IEEE Signal Processing in Medicine and Biology Symposium (SPMB), December, PA, USA, 2017.
[50] A.E. Hoerl, R.W. Kennard, Ridge regression: biased estimation for nonorthogonal problems, Technometrics 12 (February) (1970) 55–67.
[51] G. Hinton, N. Srivastava, K. Swersky, "Neural Networks for Machine Learning." pp. 29, [Online]. [Accessed: Apr. 18, 2019]. Available: http://www.cs.toronto.edu/tijmen/csc321/slides/lecture_slides_lec6.pdf.
[52] X. Glorot, Y. Bengio, Understanding the difficulty of training deep feedforward neural networks, J. Mach. Learn. Res. 9 (January) (2010) 249–256.
[53] A. Graves, Supervised Sequence Labelling with Recurrent Neural Networks, Dept. of Computer Science, University of Toronto, 2012. PhD Dissertation.
[54] Kamna Bansal, Meghana Gore, Poorna Nalabothu, "Anterior Myocardial Infarction." StatPearls [Internet], https://www.ncbi.nlm.nih.gov/books/NBK562234/ Last Update: Aug. 31, 2020, Accessed: Jan. 18, 2021.
[55] Matthew J. Warner, Vijai S. Tivakaran, "Inferior Myocardial Infarction." StatPearls [Internet], https://www.ncbi.nlm.nih.gov/books/NBK470572/#:~:text=Introduction,myocardial%20ischemia%20followed%20by%20infarction.
[56] Dipesh Ludhwani, Lovely Chhabra, Amandeep Goyal, Bryan S. Quintanilla Rodriguez, Nagendra Gupta, "Lateral Wall Myocardial Infarction." StatPearls [Internet], https://www.ncbi.nlm.nih.gov/books/NBK537228/ Last Updated: Sep. 18, 2020, Accessed: Jan. 18, 2021.
[57] Jenna M. Lizzo, Yuvraj S. Chowdhury, "Posterior Myocardial Infarction." StatPearls [Internet], https://www.ncbi.nlm.nih.gov/books/NBK553168/ Last Updated: Nov. 29, 2020, Accessed: Jan. 18, 2021.